Phototoxicity and cell passage affect intracellular reactive oxygen species levels and sensitivity towards non-thermal plasma treatment in fluorescently-labeled cancer cells

Article type: Research Article – Journal of physics D

Phototoxicity and Cell Passage Affect Intracellular Reactive Oxygen Species Levels and Sensitivity Towards Non-Thermal Plasma Treatment in Fluorescently-Labeled Cancer Cells

Hanne Verswyvel[1,2]*, Christophe Deben[1], An Wouters[1], Filip Lardon[1], Annemie Bogaerts[2], Evelien Smits[1,†], and Abraham Lin[1,2, †*]

[1] Center for Oncological Research (CORE), Integrated Personalized and Precision Oncology Network (IPPON), University of Antwerp, 2610 Antwerp-Wilrijk, Belgium.

[2] Plasma Lab for Applications in Sustainability and Medicine ANTwerp (PLASMANT), University of Antwerp, 2610 Antwerp-Wilrijk, Belgium.

[†] Shared senior author

*Correspondence

Email: hanne.verswyvel@uantwerpen.be and abraham.lin@uantwerpen.be

Abstract

Live-cell imaging with fluorescence microscopy is a powerful tool, especially in cancer research, widely-used for capturing dynamic cellular processes over time. However, light-induced toxicity (phototoxicity) can be incurred from this method, via disruption of intracellular redox balance and an overload of reactive oxygen species (ROS). This can introduce confounding effects in an experiment, especially in the context of evaluating and screening novel therapies. Here, we aimed to unravel whether phototoxicity can impact cellular homeostasis and response to non-thermal plasma (NTP), a therapeutic strategy which specifically targets the intracellular redox balance. We demonstrate that cells incorporated with a fluorescent reporter for live-cell imaging have increased sensitivity to NTP, when exposed to ambient light or fluorescence excitation, likely through altered proliferation rates and baseline intracellular ROS levels. These changes became even more pronounced the longer the cells stayed in culture. Therefore, our results have important implications for research implementing this analysis technique and are particularly important for designing experiments and evaluating redox-based therapies like NTP.

Keywords: non-thermal plasma; oxidative stress; live-cell imaging; fluorescence imaging; phototoxicity; plasma sensitivity; cell passage

Abbreviations: DBD, dielectric barrier discharge; DMEM, Dulbecco's modified Eagle medium; FBS, fetal bovine serum; GCU, green calibrated unit; GFP, green fluorescence protein; H_2O_2, hydrogen peroxide; ICD, immunogenic cell death; NTP, non-thermal plasma; RT, room temperature; RT-qPCR, quantitative real-time polymerase chain reaction; ROS, reactive oxygen species.

1 INTRODUCTION

Live-cell imaging with fluorescence microscopy is a powerful and convenient method for real-time, high-throughput capturing of dynamic cellular processes and treatment responses. This type of imaging uses *in situ* time-lapse microscopy to provide spatiotemporal visualization and quantification of living biological samples via light excitation of specific fluorophores [1]. By removing the need for fixation or dissociation of the cell culture, fluorescence live-cell imaging has advantages over other standard read-out and detection methods, including high sensitivity and selectivity, improved resolution and reproducibility, and automation and high-throughput capacities[2]. Furthermore, a wide range of fluorescence labelling techniques (e.g. chemical, enzymatic, protein/peptide tagging) are currently available, enabling the tagging of practically all subcellular compartments and structures[3, 4]. Based on application goals and biological targets, researchers can choose between transient or stable labelling of the sample. While transient labelling is ideal for rapid read-outs of monocultures, permanent incorporation of a reporter (e.g. via viral transduction or transfection), allows for the establishment of a stable fluorescent clone, thus enabling long-term analysis, screening assays, and cell tracking in relevant co-culture models[5, 6]. These appealing properties have facilitated the adoption of this versatile analytical tool in various research fields, including developmental biology, neurology, and oncology [7]. Nevertheless, a major drawback of this technique is the potential for light-induced toxicity, known as phototoxicity, which has often been drastically underestimated[8-12].

Cell cultures maintained *in vitro* are typically not adapted to coping with repetitive excitation of incorporated fluorophores by common sources of light, thus resulting in additional cellular stress, damage, or even cell death[9, 11]. Disruption of homeostasis by phototoxicity can be a major confounding factor in test samples, which negatively affects experimental read-outs and data interpretation. Even before visible indications of photodamage have occurred (e.g.

membrane blebbing, mitochondrial enlargement, cell detachment), physiological behavior can be subtly altered in response to the induced cellular stress[9].

A key factor in phototoxicity is the generation of reactive oxygen species (ROS) upon energy transfer from the light-excited fluorophore to nearby oxygen molecules[8]. In particular, recent research has shown that blue light, at intensities used to excite common fluorophores like green fluorescence protein (GFP), negatively influenced cell motility, which was directly linked to the production of the ROS, hydrogen peroxide (H_2O_2)[12]. Furthermore, quantitative real-time polymerase chain reaction (RT-qPCR) analysis demonstrated an upregulation of several antioxidant genes upon illumination[12]. Other studies concordantly reported the link between phototoxicity and redox disturbance with effects on the cell cycle, mitochondrial fragmentation, and cell migration in different cellular models[8, 10]. Therefore, acknowledging the considerable impact of phototoxicity on cellular physiology is critically needed when fluorescence live-cell imaging analysis is employed for various research applications, particularly when it is used to investigate experimental therapies, such as non-thermal plasma (NTP).

Live-cell fluorescence imaging has been a valuable tool in the field of plasma medicine for investigating cellular and subcellular NTP treatment effects for different biomedical applications, including wound healing and cancer therapy[13-16]. Mounting evidence has demonstrated that the versatile medicinal properties of NTP arise from the diverse short-lived and persistent reactive species (e.g. •OH, •NO, O/O_3, H_2O_2) that are generated [17-19]. ROS can strongly influence cellular physiology via (i) direct interaction with the plasma membrane and biochemical molecules (e.g. proteins, lipids) and/or (ii) interference with the endogenous antioxidant systems responsible for normal redox balance within the cell[20]. Moreover, the concentration of delivered ROS is determinative for biological outcome and cellular fate. Low, physiological levels of ROS are known to stimulate cell proliferation and differentiation, while higher levels are reported to induce cell cycle arrest and even cell death[21-23]. Hence, undesired ROS generation leading to phototoxicity can be a major confounding variable in the experimental evaluation of NTP treatment. This is especially problematic when the fluorescent reporter is stably integrated in the biological sample, where damage can be gradually accumulated over time and repeated cell culturing. Consequently, the potential impact of fluorescence-induced phototoxicity must be carefully evaluated in order to attribute the correct cellular effects of NTP treatment for different applications.

In this study, we investigated the effect of a stable nuclear fluorescent signaling probe, commonly used for live-cell tracking, on phototoxicity and cell response to NTP exposure. We

hypothesized that accumulating photodamage can significantly interfere with the cellular sensitivity towards NTP treatment through dysregulation of the cancer cells' redox balance. Using a virally-transduced model of the head and neck squamous cell carcinoma cell line (SC263), proliferation rates, intracellular ROS levels, and NTP treatment responses were investigated between the parental and fluorescently-transduced cells at low and high cell passages, which correspond to the cell culturing cycles and the extent to which the cells have remained in culture. Furthermore, we evaluated the sources of light (ambient light or laser-induced fluorescence excitation), which were able to interfere with cellular homeostasis. Our results indicate that fluorescent integration upon viral transduction renders cancer cells more sensitive to applied NTP treatment, especially in cells that have been extensively passaged. Remarkably, not only was fluorescence imaging able to introduce NTP sensitization in transduced cancer cells, but ambient light also had a detrimental effect. Investigation into the underlying mechanism revealed that fluorescently-transduced cancer cells exhibited significantly lower proliferation rates and elevated baseline intracellular ROS levels. These effects become more pronounced the longer the cells remain in culture. In summary, this study provides clear insights into the pathophysiological consequences of accumulating photodamage after viral transduction of fluorophores into cancer cells and suggests a direct link with increased sensitivity towards NTP *in vitro*. Therefore, this effect must be carefully considered and addressed when evaluating NTP therapy response and other redox-based therapies, in order to delineate confounding interactions and accurately draw conclusions.

2 EXPERIMENTAL METHODS

In this work, we aimed to elucidate the effect of fluorescently-labelled viral transduction on phototoxicity and cellular response to NTP therapy. The SC263 squamous cell carcinoma cell line was used and treated with a microsecond-pulsed dielectric barrier discharge (DBD) plasma system. Experiments were performed at low and high passages to further determine the effect of prolonged cell culturing. For all experiments, commercially available human cell lines were used and no ethical approvals were necessary. The SC263 cell line was kindly provided by Prof. Dr. Sandra Nuyts (University Hospital Leuven, Leuven, Belgium).

2.1 Cell Culture and Transduction

The human head and neck squamous cell carcinoma cell line, SC263, was cultured in Dulbecco's modified Eagle medium (DMEM), supplemented with fetal bovine serum (FBS) (10%), L-glutamine (1%), and penicillin/ streptomycin (1%). Cells were incubated in a

humidified atmosphere at 5% CO_2 and 37°C. Following our strict culturing method, cells were sub-cultured at 80% confluence and passaged at a 1:5 ratio every third day of culturing. Cellular autofluorescence was not observed throughout the experiments.

IncuCyte® NucLight Red Lentivirus Reagent (promoter: EF1a; fluorophore: mKate2; antibiotic selection: Puro) (4627, Essen Bioscience, Newark, United Kingdom) was used for transduction, with multiplicity of infection of 3 (MOI=3), and $>1x10^6$ transfection units (TU)/ml, and puromycin was added to select for successfully transduced cells. In order to maintaining selection of fluorescently-transduced cells, the antibiotic, puromycin, was added every 2 weeks to the cell culture. Puromycin quickly kills eukaryotic cells that do not contain this puromycin selection marker (i.e., parental cells or unsuccessfully transduced cells). The addition of puromycin was stopped at least 7 days before the start of any experiment, and fresh medium was added, to circumvent any confounding effects of the puromycin on our experimental results. This method is common practice and the recommended method for antibiotic selection[24, 25]. Following the transduction and selection process, stable red fluorescent cells (with the mKate2 fluorophore) were obtained (Figure 1a). The lentivirally-incorporated mKate2 fluorophore is the next generation of far-red fluorescent proteins, with excitation/emission maxima at 589 and 633 nm[26].

Freshly thawed cells from liquid nitrogen (P_L) and cells with a high passage (P_H), minimum of 10 extra culture cycles, from both parental (SC263) and transduced cell lines (SC263T) were seeded into 96-well plates for experiments and incubated for 24 hours before NTP treatment. Strict culturing methods and protocols were implemented to maintain an identical age between the young and older counterparts of SC263/T, respectively. This includes having exactly 2 culture passages (Px+2) over the three required replicates of each experiment. For young cell conditions, this implies experimental initiation at P2, with all experiments performed at P2+2. Once the cells exceeded 5 culture cycles, they were no longer used for the low passage number group. For the aged cellular counterparts, a minimal of 10 additional cell passages was incorporated, meaning P15 at the start of the experiment, and all experiments were completed within two additional passages (P15+2) (Figure 2).

The optimal confluence on the day of NTP treatment is between 70-75%, and the best seeding density was determined for all groups based on their growth rates (Figure 1b – Figure 1e). Here, cells were seeded at different densities and phase-contrast imaging was performed over 48 hours using the Incucyte ZOOM imaging system (Sartorius, Germany). Based on these measurements, 2.5×10^4 SC263 cells and 3.0×10^4 SC263T cells were seeded into each well, 1 day prior to NTP treatment.

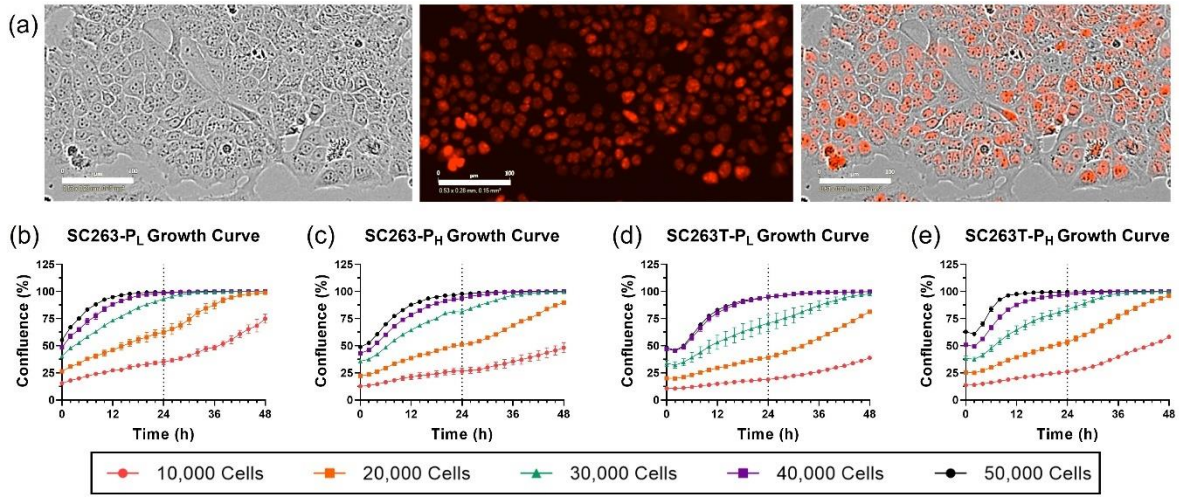

Figure 1. Fluorescently-transduced cells were seeded into 96-well plates at different densities and monitored over 48 hours to determine growth rates and optimal seeding density before NTP treatment. (a) IncuCyte® NucLight Red Lentiviral transduction and puromycin selection provided homogeneous and stable red fluorescence nuclear expression as seen in the phase contrast (left), fluorescence (middle), and merged (right) images. Images were taken by the Incucyte ZOOM® at 10x and the scale bars represent 100 µm. Confluence of non-transduced SC263 cells at (b) low passages (P_L) and (c) high passages (P_H) as well as transduced cells (SC263T) at (d) P_L and (e) P_H were also determined via live-cell image analysis using the Incucyte ZOOM® imaging system.

2.2 NTP Treatment

A microsecond-pulsed DBD system, described in our previous studies[27-30], was used for all treatments. This system consists of a microsecond-pulsed power supply (Megaimpulse Ltd, Russia) and a round-bottom dielectrically covered electrode, providing an electrically and thermally stable plasma[31]. All electrical and operation parameters are described in TABLE I. The energy per pulse of NTP, based on voltage and current waveform measurements, was calculated to be 1.8 mJ/pulse, as described in our previous report[32]. Therefore, the total NTP treatment energy was calculated to be 0.1, 0.3, 0.4, 0.9, 1.8, and 2.7 J, corresponding to the treatment times of 1, 3, 4, 10, 20, and 30 seconds.

TABLE I. Electrical & Operating Parameters of NTP Treatment

Electrical Parameters	
Pulse voltage amplitude	30 kV
Pulse rise time	1-1.5 µs
Pulse width	2 µs
Pulse frequency	50 Hz
Operating Parameters	
Application distance	1 mm
Energy per pulse	1.8 ± 0.5 mJ/pulse
Treatment time	1, 3, 4, 10, 20, and 30 s
NTP treatment energy	0.1, 0.3, 0.4, 0.9, 1.8, and 2.7 J

The microsecond-pulsed DBD system was used to treat cells in 96-well plates once 75% confluence was reached. For experiments testing the effect of ambient light, cells were taken out of the incubator and exposed to the environmental light in the cell culture hood (MSC-Advantage 1.8, ThermoFisher Scientific) for 4 hours prior to the NTP treatment (Figure 2). Cell culture medium was removed immediately before treatment and the DBD electrode was lowered into the well using a z-positioner. The electrode was fixed at 1 mm above the cells for NTP treatment, and fresh cell culture medium was added into the well right after treatment. Following treatment of all wells, the plate was incubated at 37°C and 5% CO_2 until further analysis.

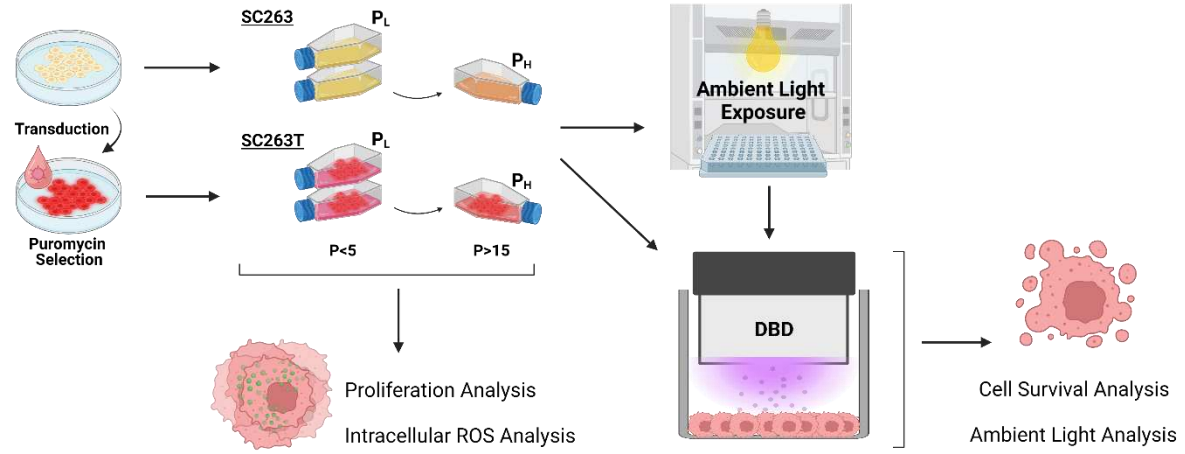

Figure 2: Schematic representation of the experimental workflow. Parental SC263 cells were virally transduced and puromycin selected to obtain a stable red-fluorescent SC263T counterpart. Freshly-thawed SC263 and SC263T cells accounted for the young cellular counterparts (P_L), whereas minimally 10 additional culture passages were performed before cells were considered for the older counterparts (P_H). Time in culture and passaging was kept identical for parental and transduced cells in both young and old counterparts, respectively, and all experiments were performed within 2 additional passages (P_x+2). To further characterize the cellular state of the different cellular conditions, proliferation and intracellular ROS level analysis was performed on all groups. Sensitivity for NTP was evaluated under standard culturing conditions, and after exposure (4 hours) to ambient light.

2.3 Cell Survival Analysis

Following NTP treatment and 24-hour incubation, 2µM of the fluorescent dye Hoechst (in 0.3% Tween, 62249, ThermoFisher Scientific) and 0.05µM of Incucyte® Cytotox Green (in DMSO, 4633, Sartorius) were added to the wells with the D300e digital dispenser (Tecan, Switzerland) for cell labeling and cell death monitoring, respectively. The working concentration for the Incucyte® Cytotox Green was previously optimized in our lab and does not induce dye cytotoxicity[30]. Brightfield and fluorescence whole-well imaging (2x) was performed with the Tecan Spark® Cyto (Green laser Ex. 461-530 nm, Blue laser Ex. 381-450 nm) after 30 minutes of incubation. All images per experiment were analyzed together using the built-in Spark Control™ Image Analyzer[33]. Briefly, whole-well analysis was performed to

ensure evaluation of the entire cell population. Focus offset (Both channels: 0mm), exposure time (Blue: 500ms; Green: 400ms), and led intensity (Blue: 60%, Green: 50%) were automatically determined with the live viewer function. Analysis masking parameters for the 2 fluorescence signals encompassed a sensitivity of 90%, with object width and length minima and maxima at 5 and 30 µm, respectively. Cell survival rates were calculated for each well (Equation 1). Live cell counts were determined by subtracting the measured dead cell counts (Green counts) from the total cell counts (Blue count). The live cell counts were then normalized to the mean of the total cell counts of the untreated condition to give the percentage of cell survival.

$$Cell\ survival\ (\%) = \frac{Blue\ Count - Green\ Count}{Mean(Blue\ Count\ Untreated)} * 100 \quad (1)$$

2.4 Proliferation Analysis

Untreated SC263 and SC263T cells were seeded into 96-well plates at 5×10^4 cells/mL (200 µL/well) to determine their baseline growth rate. Plates were monitored for 72 hours in the temperature- and CO_2- controlled Incucyte ZOOM® live-cell imaging system (37ºC and 5% CO_2). Phase contrast images (10x) were captured every 2 hours and analyzed using the Incucyte ZOOM® software to determine confluence as an indicator of cell proliferation. All images per experiment were analyzed together using the same image analysis parameters to reduce variability.

2.5 Intracellular ROS Analysis

In order to determine the baseline redox status of untreated SC263 and SC263T cells, the intracellular ROS levels were measured. Cells were seeded into 96-well plates at 5×10^4 cells/mL (200 µL/well) and incubated at 37ºC and 5% CO_2 overnight to allow for cell attachment. Following incubation, the medium was removed and replaced with fresh medium containing 2.5 µM CellROX™ Green Reagent (C10444, ThermoFisher Scientific). This cell-permeant dye, upon oxidation, binds to DNA and exhibits photostable fluorescence with excitation and emission maxima at 485 and 520 nm, respectively. After 30 minutes of incubation, baseline intracellular ROS levels were obtained with the Incucyte ZOOM® imaging system (Green laser Ex./Em.: 441-481/503-544 nm)[34]. Fold change of mean green fluorescence (green calibrated unit; GCU) was calculated for both transduced and parental cells at low and high passages.

For the assessment of ROS induction after repetitive fluorescent excitation, cells were prepared as described above. Phase contrast and fluorescence images were captured every 2 hours up to 48 hours in the Incucyte ZOOM® live-cell imaging system and the intracellular ROS level was measured with CellROX™. Analysis was performed using the Incucyte ZOOM® software and mean GCU was measured following background subtraction and thresholding. All images per experiment were analyzed together using the same image analysis parameters to limit variability.

2.6 Statistical Analysis

For kinetic, live-cell imaging analysis, statistical significance was determined using a Two-Way ANOVA. The mean values of the cell lines (confluence or GCU) were compared to each other at each specific time point. A Tukey test was performed to correct for multiple comparisons. For baseline intracellular ROS levels, fold change of the mean GCU was calculated and a One-Way ANOVA with a Dunn's multiple comparisons test was used to determine significance. For the analysis of intracellular ROS levels over time, statistical significance was determined using a mixed-effect analysis. The mean GCU values of the cell lines were compared to each other at each time point and a Holm-Sidak's multiple comparison test was performed. Data in the figures are presented as mean ± standard error of the mean (SEM).

3 RESULTS

3.1 Fluorescently-Transduced Cells Acquire Increased Sensitivity to NTP

To determine the effects of fluorescence-induced photodamage on NTP therapy response, both the parental (SC263) and fluorescently-transduced (SC263T) cell lines were treated with NTP and analyzed 24 hours later for cell survival. While no significant differences in NTP sensitivity were observed between the SC263T cell line (SC263T-P_L) and the parental cells at low passages (SC263-P_L) (Figure 3a), at higher passages (P_H), the SC263T-P_H cells became more sensitive to NTP compared to their parental counterpart (Figure 3b). At NTP treatments of 0.4 J and higher, cellular survival was reduced in the SC263T-P_H group compared to parental SC263-P_H, within the same treatment condition ($p \leq 0.003$). Indeed, it is apparent that non-transduced SC263 cells retained their original sensitivity to NTP, regardless of how long they remained in culture (Figure 3c), thus suggesting the absence of genetic drift/instability or selection pressures resulting in phenotypic changes. However, following continuous

culturing, the transduced SC263T-P_H cells became more sensitive to NTP compared to their early passage counterparts, SC263T-P_L (Figure 3d). Quantification of transduced cancer cell survival showed that with higher passages, NTP treatment at 0.9 J and higher, further decreased cell viability by 12% compared to the lower passage cells ($p = 0.0135$).

In summary, our results revealed that viral transduction for live-cell imaging renders cancer cells more sensitive to applied NTP treatment, following prolonged cell culture and passaging. In the following experiments, we aimed to investigate which sources of light could introduce these sensitizing effects.

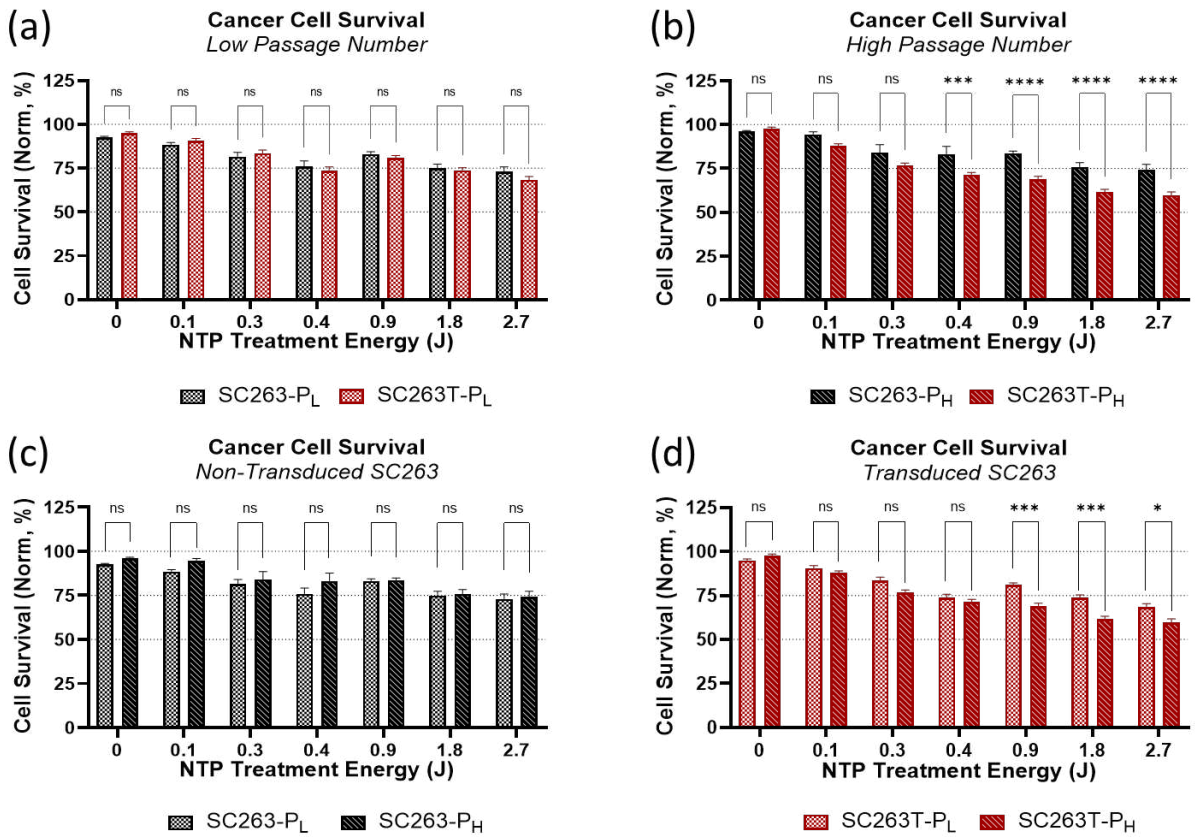

Figure 3. Cancer cell survival analysis 24 hours after different NTP treatment energies. (a) At low passages, no significant differences in NTP sensitivity were reported between the transduced (SC263T) and parental cells (SC263), while after higher passages (b), transduced SC263T-P_H cells showed significantly reduced survival following NTP treatment at 0.4 J and higher, compared to the non-transduced counterparts. (c) The passaging of parental SC263 cells did not affect their sensitivity to NTP, but in contrast, (d) NTP sensitivity increased in the transduced cells, with significantly lower survival rates in the SC263T-P_H compared to SC263T-P_L at 0.9 J of NTP treatment energy and higher. Data are presented as mean±SEM of 3 independent repeats (n=15-20). Statistical significance was determined with a Two-Way ANOVA and a post hoc Tukey's multiple comparison test. * $p \leq 0.05$, *** $p \leq 0.001$, **** $p \leq 0.0001$.

3.2 Phototoxicity from Different Light Sources Affects NTP Treatment Response and Cellular Physiology

To investigate which types of light excitation were able to induce the observed phototoxicity and increased NTP sensitivity, both parental and fluorescently-transduced cell

lines were exposed to ambient light before NTP treatment, and analyzed for cell survival, 24 hours post NTP exposure. The effects of temperature changes (37°C vs room temperature, RT) were taken into account and did not affect cell survival (Appx A). Prolonged exposure to ambient light did not render the parental cells more sensitive to NTP treatment (Figure 4a). However, transduced SC263T showed increased sensitivity towards NTP application after ambient light exposure (Figure 4b), and at the high treatment energy of 2.7 J, caused significantly increased cell death ($p = 0.0325$). Here, these observations are in accordance with the findings for the SC263T-P_H (Figure 3d) prolonged cell culturing and passaging exposed cells to more ambient light compared to their earlier counterparts.

Another contributing factor of phototoxicity is repetitive exposure by an excitation laser in time-lapse imaging. To investigate whether this could also affect cellular physiology, we evaluated intracellular ROS levels in cells following repetitive scanning. Over the course of imaging, the intracellular ROS levels of the SC263T cell line became significantly higher compared to their non-transduced counterparts for both low ($p = 0.0444$) and high passages ($p = 0.0007$), which persisted for 48 hours (Figure 4c,d). Moreover, intracellular ROS levels increased more with higher passages; starting from 28 hours, the SC263T-P_H cell line exhibited significantly higher intracellular ROS levels than the SC263T-P_L cell line ($p \leq 0.05$), while no differences were measured between the low and high passaged, parental cell line ($p > 0.05$).

In summary, our results reveal that fluorescence-induced phototoxicity can originate from different sources of light, whereby cellular physiology and treatment response can be affected. This includes both ambient light in the work environment, as well as laser excitation from time-lapse imaging studies. In the following experiments, we aimed to further investigate the underlying mechanisms of increased NTP sensitivity in transduced cancer cells.

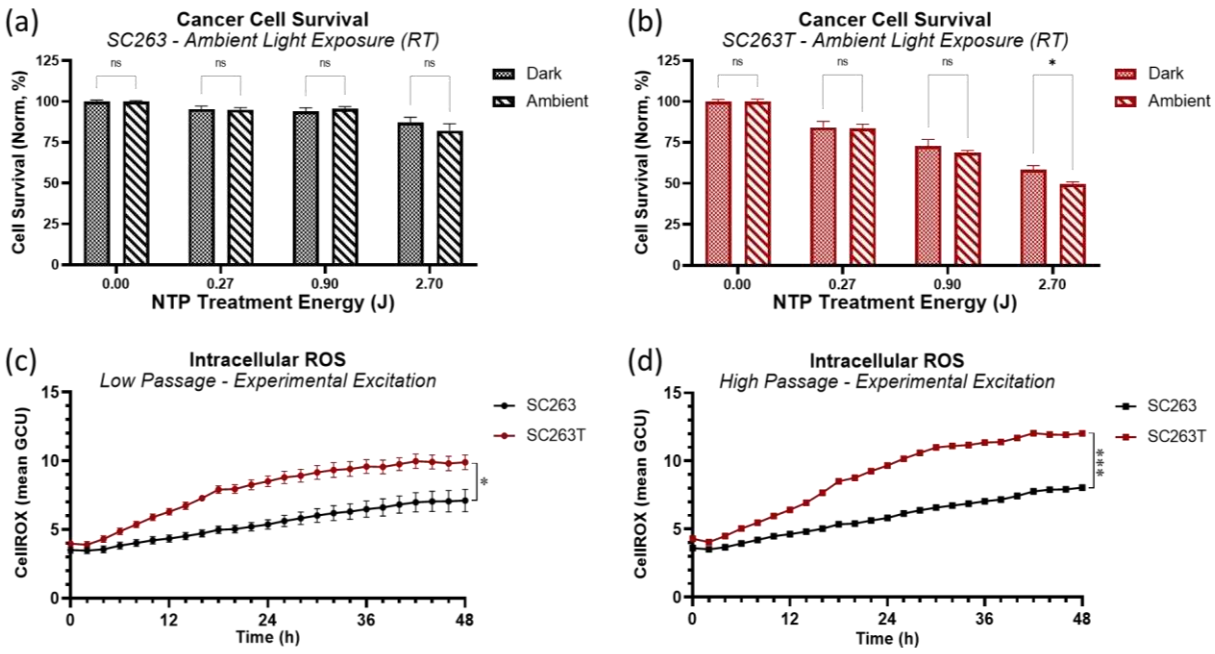

Figure 4. Light excitation from different sources results in altered NTP responses and cellular physiology. (a) After exposure to ambient light, no significant differences in NTP sensitivity were reported for parental cells (SC263), compared to cells incubated in the dark. (b) In contrast, transduced cells (SC263T) became more sensitive to high NTP treatment energy following prolonged ambient light exposure. (c) Repetitive, time-lapse imaging significantly elevated intracellular ROS levels in SC263T-P_L cells compared to parental SC263-P_L cells, (d) which became more pronounced over increased passaging. Data are presented as mean±SEM of 3 independent repeats (n=15). Statistical significance was determined with a Two-Way ANOVA and a post hoc Tukey's multiple comparison test for cell survival analysis; a mixed-effect model and the Holm-Sidak's multiple comparison test was used for the assessment of intracellular ROS levels. * $p \leq 0.05$, *** $p \leq 0.001$.

3.3 Fluorescently-Transduced Cells Acquire a Lower Rate of Proliferation and Higher Baseline Intracellular ROS Levels

It has been hypothesized that NTP therapy can preferentially target fast-proliferating cells, and therefore, we tested whether the increased NTP sensitivity of the SC263T-P_H cell line was due to higher growth rates compared to the other cell counterparts.

The cells were seeded into 96-well plates and monitored for 72 hours with phase contrast live-cell imaging. Interestingly, the non-transduced cell lines, regardless of low or high passages, proliferated at a faster rate compared to the transduced cell lines (Figure 5a). Quantification of cell confluence revealed that following transduction, cell proliferation was significantly reduced (Figure 5b). Indeed, even for low passages, fluorescence transduction affected cell growth compared to that of the parental cells (SC263T-P_L vs SC263-P_L; $p = 0.003$). This effect was even more pronounced the longer the cells stayed in culture (SC263T-P_H vs SC263-P_H; $p < 0.0001$). This was even more clearly evidenced as cell passage did not significantly affect growth of non-transduced cell lines, while significant differences were measured between low and high passaged transduced cell lines (SC263T-P_L vs SC263T-P_H; $p < 0.0001$).

Taken together, it is clear that following fluorescent transduction, the proliferation rate was significantly affected early after transduction and further reduced after continuous culturing. Here, it does not appear that the higher sensitivity to NTP treatment is due to a faster proliferation rate, as previously hypothesized in literature.

Another prevalent hypothesis for why certain cells are more sensitive to NTP therapy is based on their ability to balance their cellular redox status[28, 29]. It has been hypothesized that certain cells have higher baseline intracellular ROS levels, and therefore delivery of additional ROS from NTP treatment leads to irreversible oxidative distress and damage. Therefore, we aimed to investigate whether the more sensitive SC263T-P_H cells had elevated baseline intracellular ROS levels compared to their parental counterparts.

Baseline ROS levels of the cell lines were evaluated with CellROX^{TM} Green Reagent (2.5 µM) and a single-timepoint analysis. It is clear that the SC263T-P_H cells exhibited higher fluorescence intensity compared to all other cell counterparts, thus indicating higher levels of intracellular ROS (Figure 5c). The mean fluorescence intensity was quantified using the Incucyte ZOOM® live-cell analysis software and fold changes ware calculated between parental and transduced counterparts (Figure 5d), and revealed that baseline intracellular ROS levels in transduced SC263T cells were significantly higher compared to the parental cells for both low (0.15 ± 0.03 fold; p = 0.0079) and high passages (0.21 ± 0.03 fold; p = 0.0001). Furthermore, following continuous culturing, the transduced SC263T-P_H cells displayed a signficant further elevation in basal ROS levels compared to their younger counterpart, SC263T-P_L (Appx B).

Taken together, it appears that baseline intracellular ROS levels increased following fluorescence transduction, which could partially contribute to redox disregulation and NTP sensitization. Moreover, in the context of NTP treatment, while cell survival was not affected by fluorescence transduction at low cell passages (Figure 3a), these data highlight that there are already early changes to cellular physiology (Figure 5b, d), which must be carefully considered in the experimental design.

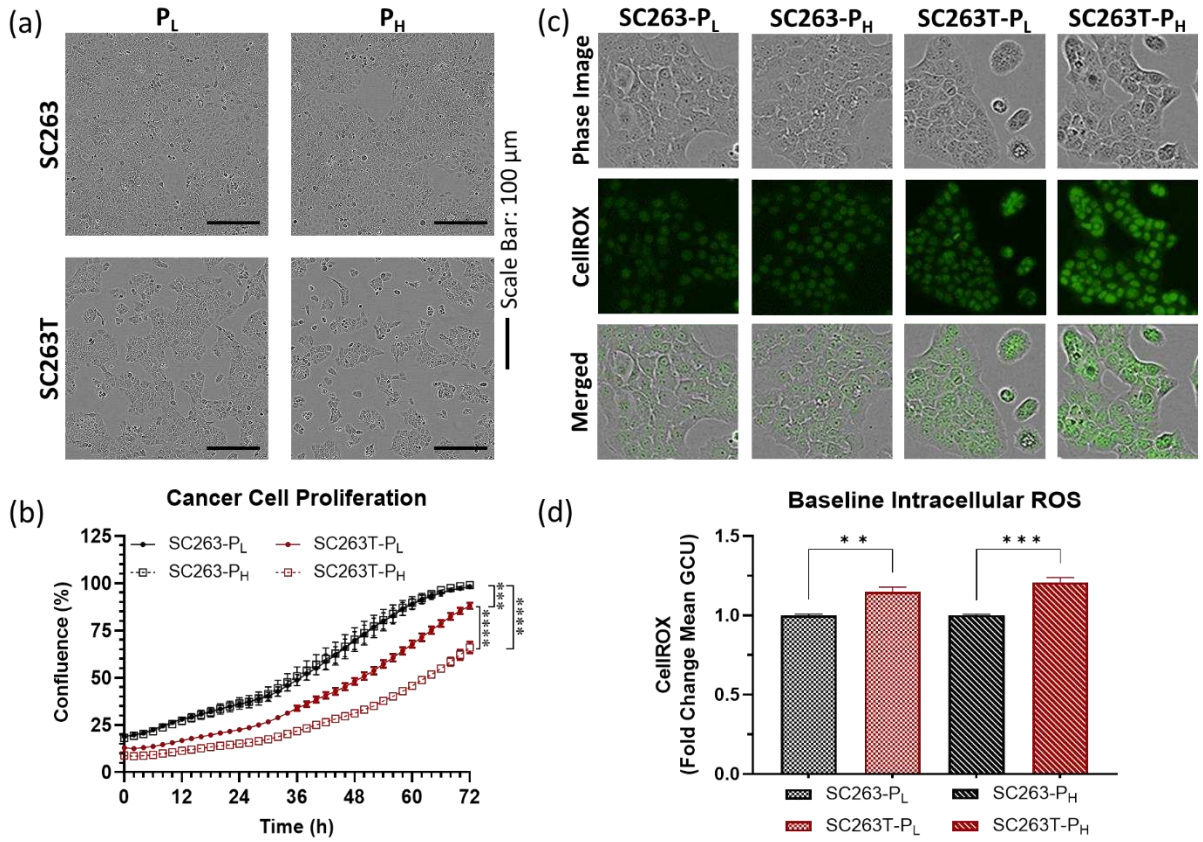

Figure 5. Cancer cell proliferation and basal ROS level analysis. (a) Phase contrast images taken at 10x show that non-transduced cell lines, regardless of low or high passage, were more confluent at 72 h compared to their transduced counterparts. Scale bar indicates 300 µm. (b) Quantification of cell confluence revealed that the growth rates of the non-transduced cell line (SC263) remained unchanged at low (P_L) and high passages (P_H), while a significant difference was observed in the transduced cell line (SC263T). (c) Phase contrast and fluorescence images captured at 10x revealed that the high-passaged, transduced cell line (SC263T-P_H) exhibited the highest fluorescence intensity at basal level. (d) Quantification of the mean green fluorescence intensity of the images (GCU) indicate that following transduction, intracellular ROS levels increased and continued to increase with higher passages. Data are represented as mean±SEM of 3 independent repeats (n=10-15). Statistical significance was determined using a Two-Way ANOVA and a post hoc Tukey's multiple comparison test for the proliferation assay; a One-Way ANOVA with a Dunn's multiple comparisons test was used to assess basal intracellular ROS level significance. ** $p \leq 0.01$, *** $p \leq 0.001$, ****$p \leq 0.0001$.

4 DISCUSSION AND CONCLUSION

In this study, we investigated the cellular effects of accumulating phototoxicity in living samples after introduction of a stable fluorescent reporter and demonstrated a significant impact on the growth potential and intracellular redox balance. This was accompanied with an increase in sensitivity towards NTP treatment and has broader impacts to other redox-based therapy evaluations using similar analysis techniques.

To date, the effect of fluorescence viral transduction and cellular response to NTP therapy has not yet been investigated. In that regard, we performed a comprehensive study between parental SC263 cells and their transduced counterpart, incorporated with a fluorescent reporter (Figure 1). Based on cancer cell survival quantification (Figure 3b), we observed that

the cells most sensitive to NTP were the transduced cells after prolonged passaging (SC263T-P_H). This suggested that accumulation of fluorescence-induced phototoxicity was able to modulate cellular susceptibility to NTP and thereby confound experimental results. Further insight into the sources of light that induce fluorescence-associated phototoxicity revealed that both ambient light in the working environment as well as laser excitation in time-lapse experiments, were able to interfere with cellular redox homeostasis and induce NTP sensitization (Figure 4). More detailed investigation into the underlying cause revealed that the enhanced responsiveness to NTP was not associated with changes in cellular morphology or a higher proliferative capacity, as previously suggested in literature, but potentially with a higher baseline intracellular ROS level (Figure 5, Appendix C). It is important to note that cytotoxicity from the fluorescent dyes used here was considered negligible, as the working concentrations were previously optimized and high cell survival was demonstrated for untreated controls in every experiment (SC263/T-P_L/P_H).

In addition to reactive chemical species being generated by NTP, different physical factors, including electric fields, ultraviolet (UV) radiation, and thermal changes, are produced. These physical factors could also interact with, and influence the biological samples during NTP treatment, especially with the DBD system. In the past, detailed electrical and energy characterizations of DBD devices were performed by different labs, including our lab with our device, to ensure the delivery of an electrically and thermally stable plasma[31, 32, 35, 36]. In addition, several studies have already demonstrated that neither global and local electric fields, nor physical factors (e.g. UV radiation, thermal damage) originating from NTP treatment contribute to the induction of cell death[37-39]. Indeed, Lin et al., have reported that DBD plasma discharged in pure nitrogen did not induce cell death for multiple cancer types. In this setting, cells were exposed to UV radiation, global pulsed-electric fields, and local electric fields and temperature changes from streamers and filaments[37, 38]. Taken together, it was clear that the reactive oxygen species were the main biological effectors, and in our similar system, theses physical components had minimal effect on cancer cell death.

It has long been hypothesized that increased vulnerability of certain cells towards NTP is a result of different cell types displaying a diverse range of redox profiles. In fact, certain cancer cells exhibit higher intracellular ROS levels at a basal state and consequently live in a permanent state of oxidative stress[40]. It was stated that such cells are the first to reach the threshold of damaging redox imbalance when challenged with exogenous sources of reactive species, thereby rendering them more prone to therapies like NTP[20, 40-42]. Here, we have demonstrated that the more sensitive SC263T cells had elevated intracellular ROS levels after

fluorophore incorporation, which became more pronounced over time (Figure 5). Hence, inherent elevation of intracellular oxidative stress, caused by the fluorescence-induced reactive photodamage, could be part of the reason why transduced cancer cells exhibit increased susceptibility to NTP. Of note, a growing body of evidence has indicated that ROS production is intertwined with metabolic changes in cancer cells, and thus, the first studies investigating the link between NTP treatment responsiveness and tumor cell metabolism are emerging[15, 43]. Therefore, it cannot be ruled out that significant metabolic dysregulation, linked to higher intracellular ROS levels, is a contributing factor to the observed changes in NTP vulnerability and this paradigm requires further investigation. Investigation into more specific ROS subtypes, distribution within the cell, and subsequent engagement of defensive antioxidant systems may provide further clarification of the NTP sensitization effects [44, 45].

The results of the findings presented here highlight several important considerations when designing live-cell imaging experiments to investigate NTP therapy and other redox-based treatments. Since phototoxicity can be accumulated over time, researchers implementing fluorescence live-cell imaging should carefully evaluate when transduced cells diverge from their parental counterparts. This could then be partially avoided by limiting the number of passaging events and reducing the time transduced cells are in culture. Indeed, our cell physiology data complement our findings that high-passaged transduced cells were more sensitive to NTP, as with prolonged passaging, they would incur more photodamage from handling in working environments. In addition, detailed fluorochrome selection, reduction of scanning intensity, and limiting the number of image acquisition events would limit laser-induced phototoxicity during time-lapse experiments. Another option is to opt for the use of transient fluorescence dyes, where cells are only tagged before an experiment and not during maintenance of the cell culture. Although the fluorescence expression from this incorporation method is typically less stable compared to more integrated techniques, such as viral transduction, it helps reduce the acquired biological variance from potential prolonged phototoxicity. These considerations should not only be taken into account for experiments utilizing 2D monolayer cultures demonstrated here, but also for those using 3D *in vitro* models. Moreover, immunofluorescence is also used in *in vivo* research for tracking tumor growth in orthotopic models and follow-up of metastasis[46, 47]. Although ambient light is not a confounding factor *in situ* in the *in vivo* environment, our findings could have important implications to take into account during preparatory cell culturing and experimental handling prior to tumor cell inoculation.

Taken together, our study reports a significant impact of stable fluorescence transduction and prolonged culturing on cellular behavior, physiology, and NTP treatment responsiveness. Although imaging-associated phototoxicity has already been discussed in literature, we report a direct link between the introduction of a fluorescence reporter and alterations in sensitivity to NTP application. These results have important, broader implications for research into other treatment strategies focusing on dysregulating the cancer cell's redox balance, and should be further extrapolated to other cell, cancer, and fluorescent reporter types in future studies. Therefore, although fluorescence live-cell imaging is a powerful research technique, delineating the confounding effects associated with phototoxicity is absolutely critical, in order to draw the correct conclusions.

ACKNOWLEDGMENTS

This work was partially funded by the Research Foundation – Flanders (FWO) and supported by the following grants: 1S67621N (H.V.), 12S9221N (A.L.), and G044420N (A.B. and A.L.). We would also like to thank several patrons, as part of this research was funded by donations from different donors, including Dedert Schilde vzw, Mr Willy Floren, and the Vereycken family.

AUTHOR CONTRIBUTIONS

H.V. Conceptualization (equal); data curation (lead); formal analysis (lead); funding acquisition (equal); investigation (lead); methodology (lead); validation (lead); visualization (lead); writing – original draft (lead); writing – review and editing (lead). **C.D.** Methodology (supporting); resources (equal); writing – review and editing (supporting). **A.W.** Methodology (supporting); resources (equal); writing – review and editing (supporting). **F.L.** Funding acquisition (equal); project administration (equal); resources (equal); writing – review and editing (supporting). **A.B.** Funding acquisition (equal); project administration (equal); resources (equal); supervision (equal); writing – original draft (supporting); writing – review and editing (supporting). **E.S.** Funding acquisition (equal); project administration (equal); resources (equal); supervision (equal); writing – original draft (supporting); writing – review and editing (supporting). **A.L.** Conceptualization (equal); funding acquisition (equal), data curation (supporting); formal analysis (supporting); methodology (supporting); project administration (equal); supervision (equal); writing – original draft (supporting); writing – review and editing (supporting).

CONFLICT OF INTEREST

The authors declare no financial or commercial conflict of interest.

DATA AVAILABILITY STATEMENT

The data that support the findings of this study are available from the corresponding author upon reasonable request.

REFERENCES

1. Ettinger, A. and T. Wittmann, *Chapter 5 - Fluorescence live cell imaging*, in *Methods in Cell Biology*, J.C. Waters and T. Wittman, Editors. 2014, Academic Press. p. 77-94.
2. Martinez, N.J., et al., *High-throughput fluorescence imaging approaches for drug discovery using in vitro and in vivo three-dimensional models.* Expert Opin Drug Discov, 2015. **10**(12): p. 1347-61.
3. Schneider, A.F.L. and C.P.R. Hackenberger, *Fluorescent labelling in living cells.* Curr Opin Biotechnol, 2017. **48**: p. 61-68.
4. Toseland, C.P., *Fluorescent labeling and modification of proteins.* Journal of chemical biology, 2013. **6**(3): p. 85-95.
5. Galas, L., et al., *"Probe, Sample, and Instrument (PSI)": The Hat-Trick for Fluorescence Live Cell Imaging.* Chemosensors, 2018. **6**(3): p. 40.
6. Chudakov, D.M., et al., *Fluorescent Proteins and Their Applications in Imaging Living Cells and Tissues.* Physiological Reviews, 2010. **90**(3): p. 1103-1163.
7. Dean, K.M. and A.E. Palmer, *Advances in fluorescence labeling strategies for dynamic cellular imaging.* Nature Chemical Biology, 2014. **10**(7): p. 512-523.
8. Dixit, R. and R. Cyr, *Cell damage and reactive oxygen species production induced by fluorescence microscopy: effect on mitosis and guidelines for non-invasive fluorescence microscopy.* Plant J, 2003. **36**(2): p. 280-90.
9. Icha, J., et al., *Phototoxicity in live fluorescence microscopy, and how to avoid it.* Bioessays, 2017. **39**(8).
10. Kiepas, A., et al., *Optimizing live-cell fluorescence imaging conditions to minimize phototoxicity.* J Cell Sci, 2020. **133**(4).
11. Laissue, P.P., et al., *Assessing phototoxicity in live fluorescence imaging.* Nature Methods, 2017. **14**(7): p. 657-661.
12. Alghamdi, R.A., et al., *Assessing Phototoxicity in a Mammalian Cell Line: How Low Levels of Blue Light Affect Motility in PC3 Cells.* Frontiers in cell and developmental biology, 2021. **9**: p. 738786.
13. Van Loenhout, J., et al., *Cold Atmospheric Plasma-Treated PBS Eliminates Immunosuppressive Pancreatic Stellate Cells and Induces Immunogenic Cell Death of Pancreatic Cancer Cells.* Cancers, 2019. **11**(10): p. 1597.
14. Van Loenhout, J., et al., *Auranofin and Cold Atmospheric Plasma Synergize to Trigger Distinct Cell Death Mechanisms and Immunogenic Responses in Glioblastoma.* Cells, 2021. **10**(11): p. 2936.
15. Trzeciak, E.R., et al., *Oxidative Stress Differentially Influences the Survival and Metabolism of Cells in the Melanoma Microenvironment.* Cells, 2022. **11**(6): p. 930.
16. Kupke, L.S., et al., *Cold Atmospheric Plasma Promotes the Immunoreactivity of Granulocytes In Vitro.* Biomolecules, 2021. **11**(6): p. 902.
17. Lin, A., et al., *Non-Thermal Plasma as a Unique Delivery System of Short-Lived Reactive Oxygen and Nitrogen Species for Immunogenic Cell Death in Melanoma Cells.* Advanced Science, 2019. **6**(6): p. 1802062.
18. Yan, D., J.H. Sherman, and M. Keidar, *Cold atmospheric plasma, a novel promising anti-cancer treatment modality.* Oncotarget, 2016. **8**(9): p. 15977-15995.
19. Tanaka, H., et al., *Molecular mechanisms of non-thermal plasma-induced effects in cancer cells %J Biological Chemistry.* Biological Chemistry, 2019. **400**(1): p. 87-91.
20. Van Loenhout, J., et al., *Oxidative Stress-Inducing Anticancer Therapies: Taking a Closer Look at Their Immunomodulating Effects.* Antioxidants (Basel), 2020. **9**(12).
21. Kalghatgi, S., et al., *Endothelial cell proliferation is enhanced by low dose non-thermal plasma through fibroblast growth factor-2 release.* Ann Biomed Eng, 2010. **38**(3): p. 748-57.

22. Tan, F., et al., *Controlling stem cell fate using cold atmospheric plasma.* Stem Cell Research & Therapy, 2020. **11**(1): p. 368.
23. Kim, C.H., et al., *Induction of cell growth arrest by atmospheric non-thermal plasma in colorectal cancer cells.* J Biotechnol, 2010. **150**(4): p. 530-8.
24. Kallifatidis, G., et al., *Improved lentiviral transduction of human mesenchymal stem cells for therapeutic intervention in pancreatic cancer.* Cancer Gene Therapy, 2008. **15**(4): p. 231-240.
25. Xuan, F., et al., *MINA53 deficiency leads to glioblastoma cell apoptosis via inducing DNA replication stress and diminishing DNA damage response.* Cell Death Dis, 2018. **9**(11): p. 1062.
26. Bioquest, A., *Spectrum [mKate2].* 2021.
27. Lin, A., et al., *Critical Evaluation of the Interaction of Reactive Oxygen and Nitrogen Species with Blood to Inform the Clinical Translation of Nonthermal Plasma Therapy.* Oxidative Medicine and Cellular Longevity, 2020. **2020**: p. 9750206.
28. Lin, A., et al., *Oxidation of Innate Immune Checkpoint CD47 on Cancer Cells with Non-Thermal Plasma.* Cancers, 2021. **13**(3): p. 579.
29. Lin, A., et al., *The effect of local non-thermal plasma therapy on the cancer-immunity cycle in a melanoma mouse model.* 2022. **n/a**(n/a): p. e10314.
30. Lin, A., et al., *Acquired non-thermal plasma resistance mediates a shift towards aerobic glycolysis and ferroptotic cell death in melanoma.* Drug Resistance Updates, 2023. **67**: p. 100914.
31. Lin, A., et al., *The effect of local non-thermal plasma therapy on the cancer-immunity cycle in a melanoma mouse model.* Bioengineering & Translational Medicine, 2022. **7**(3): p. e10314.
32. Lin, A., et al., *Toward defining plasma treatment dose: The role of plasma treatment energy of pulsed-dielectric barrier discharge in dictating in vitro biological responses.* Plasma Processes and Polymers, 2022. **19**(3): p. e2100151.
33. Tecan, *THE SPARK® MULTIMODE MICROPLATE READER - YOUR RESEARCH PARTNER.* 2023.
34. Scientific, T., *Fluorescence SpectraViewer.*
35. Kalghatgi, S.U., et al. *Non-thermal dielectric barrier discharge plasma treatment of endothelial cells*. in *2008 30th Annual International Conference of the IEEE Engineering in Medicine and Biology Society*. 2008.
36. Wende, K., A. Schmidt, and S. Bekeschus, *Safety Aspects of Non-Thermal Plasmas*, in *Comprehensive Clinical Plasma Medicine: Cold Physical Plasma for Medical Application*, H.-R. Metelmann, T. von Woedtke, and K.-D. Weltmann, Editors. 2018, Springer International Publishing: Cham. p. 83-109.
37. Lin, A., et al., *Non-Equilibrium Dielectric Barrier Discharge Treatment of Mesenchymal Stem Cells: Charges and Reactive Oxygen Species Play the Major Role in Cell Death.* Plasma Processes and Polymers, 2015. **12**(10): p. 1117-1127.
38. Lin, A., et al., *Nanosecond-Pulsed DBD Plasma-Generated Reactive Oxygen Species Trigger Immunogenic Cell Death in A549 Lung Carcinoma Cells through Intracellular Oxidative Stress.* International Journal of Molecular Sciences, 2017. **18**(5): p. 966.
39. Lin, A., et al., *Non-Thermal Plasma as a Unique Delivery System of Short-Lived Reactive Oxygen and Nitrogen Species for Immunogenic Cell Death in Melanoma Cells.* Advanced Science, 2019. **0**(0): p. 1802062.
40. Liou, G.-Y. and P. Storz, *Reactive oxygen species in cancer.* Free radical research, 2010. **44**(5): p. 479-496.
41. Perillo, B., et al., *ROS in cancer therapy: the bright side of the moon.* Experimental & Molecular Medicine, 2020. **52**(2): p. 192-203.

42. Trzeciak, E.R., et al., *Oxidative Stress Differentially Influences the Survival and Metabolism of Cells in the Melanoma Microenvironment.* 2022. **11**(6): p. 930.
43. Bekeschus, S., et al., *Tumor cell metabolism correlates with resistance to gas plasma treatment: The evaluation of three dogmas.* Free Radic Biol Med, 2021. **167**: p. 12-28.
44. Schieber, M. and N.S. Chandel, *ROS function in redox signaling and oxidative stress.* Curr Biol, 2014. **24**(10): p. R453-62.
45. Snezhkina, A.V., et al., *ROS Generation and Antioxidant Defense Systems in Normal and Malignant Cells.* Oxid Med Cell Longev, 2019. **2019**: p. 6175804.
46. Moreno, J.A., et al., *Fluorescent Orthotopic Mouse Model of Pancreatic Cancer.* J Vis Exp, 2016(115).
47. Yuzhakova, D., et al., *Highly Invasive Fluorescent/Bioluminescent Patient-Derived Orthotopic Model of Glioblastoma in Mice.* Frontiers in Oncology, 2022. **12**.

APPENDIX A

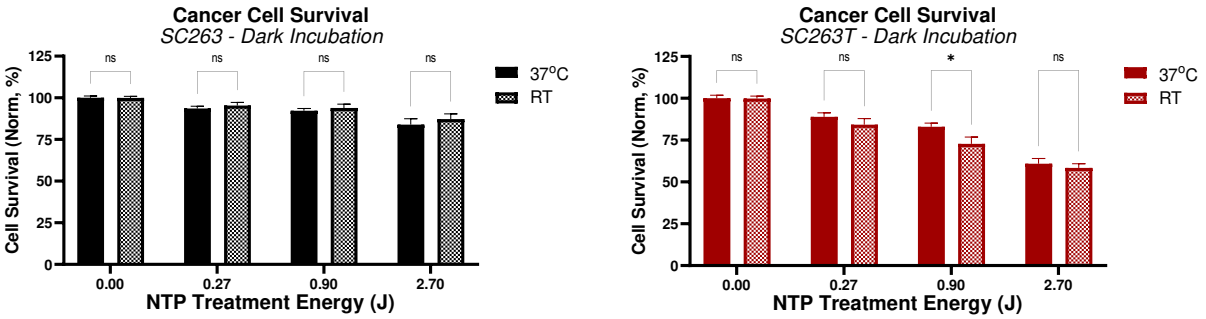

Cell Survival analysis 24 hours post NTP exposure after incubation at different temperatures. To perform ambient light-exposure experiments, effects of changes in incubation temperature needed to be taken into account. Overall, cell survival after NTP treatment was not or minimally affected by this environmental change, for both parental as transduced SC263 cells. Statistical significance was determined with a Two-Way ANOVA and a post hoc Tukey's multiple comparison test. * $p \leq 0.05$.

APPENDIX B

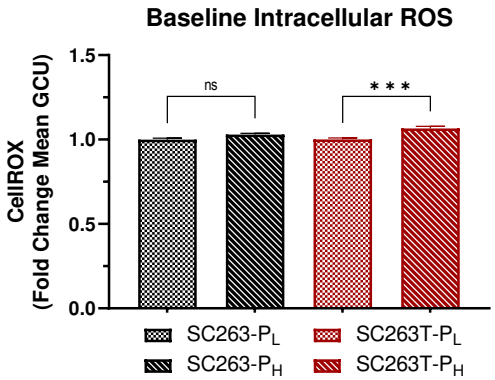

Baseline intracellular ROS level comparison between low- and high-passaged cellular counterparts. Quantification of the mean green fluorescence intensity of the images (GCU) and calculation of fold changes between young and older counterparts showed that continuous culturing had no effect on basal ROS levels in the parental cell lines. In contrast, a significant elevation of baseline ROS levels in the transduced cell line following prolonged passaging (SC263T-P_H) was observed, compared to their younger counterpart SC263T-P_L. Data are represented as mean±SEM of 3 independent repeats (n=10-15). Statistical significance was determined using a One-Way ANOVA with a Dunn's multiple comparisons test. *** $p \leq 0.001$.

APPENDIX C

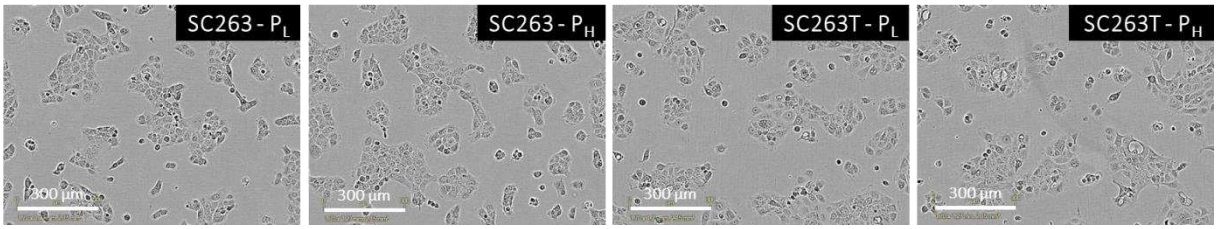

Cellular morphology of the different cellular counterparts in culture. Appearance of the cells was closely monitored, and compared between the different cellular counterparts (SC263/T - P_L/P_H). Phenotypical changes were not observed throughout the course of the experiments.